THE EFFECT OF REHEATING TEMPERATURE ON THE DISSOLUTION OF PRECIPITATES AND MECHANICAL PROPERTIES OF MICROALLOYED STEEL HEAVY PLATES*

Fábio Dian Murari[1]
Antônio Adel dos Santos[2]
André Luiz Vasconcellos da Costa e Silva[3]
José María Rodriguez-Ibabe[4]

Abstract
The effect of reheating temperature of slabs on the precipitates dissolution and mechanical properties of Ti-Nb microalloyed steel was investigated in pilot scale. It was verified, by means of transmission electron microscopy, a significant decrease in precipitates formed during the solidification of the steel as the reheating temperature increased from 1100°C to 1200°C. No significant changes in size and shape of the precipitates were observed with further temperature increase up to 1280°C. In line with the precipitates dissolution behavior, an increase in strength was observed with the elevation of the reheating temperature up to 1200°C, due in part to the reprecipitation of fine Nb-rich precipitates during the hot rolling. At 1200°C the presence of deformed ferrite on the microstructure contributed to the additional increase in strength. After reheating above 1200°C up to 1280°C, a decrease in strength of the rolled plates was noticed. This effect has been credited to the absence of deformed ferrite grains and also to a small increase in the low angle grain boundaries size. The results were in agreement with Thermo-Calc and Dictra simulations.
Keywords: Reheating plates; Precipitates dissolution; Heavy plates.

[1] *Metallurgical Engineer, D. Sc., Specialist Researcher, Usiminas Research Center, Ipatinga, MG, Brazil.*
[2] *Metallurgical Engineer, D. Sc., Senior Specialist Researcher, Usiminas Research Center, Ipatinga, MG, Brazil..*
[3] *Metallurgical Engineer, PhD, Associate Professor, Department of Metallurgy and Materials,Universidade Federal Fluminense, Volta Redonda, RJ, Brazil.*
[4] *Industrial Engineer, Dr.-Eng.; Senior Researcher, CEIT, Donostia-San Sebastian, Spain.*

** Technical contribution to the 11th International Rolling Conference, part of the ABM Week 2019, October 1st-3rd, 2019, São Paulo, SP, Brazil.*

1 INTRODUCTION

The initial stage of any hot deformation process is the reheating of the material. The objective of this step is to raise the temperature to give the necessary plasticity for the hot deformation and to dissolve the precipitates of existing microalloying elements in order to guarantee the precipitation of fine particles in the metallic matrix during hot rolling and/or cooling of the plate [1-3].

Among the main microalloying elements used, Nb is considered the most important. It plays a fundamental role in the majority of steels processed as heavy plates because it allows obtaining a final refined microstructure, resulting in an excellent combination of mechanical resistance and toughness properties. In addition to the grain refining effect, Nb also contributes to increasing the strength properties by means of the precipitation hardening mechanism. However, in order to play its full potential, the Nb added into the steel must be dissolved in the matrix in the end of reheating, on slab discharging [4,5].

During continuous casting of Ti-Nb microalloyed steels, coarse (Ti,Nb)(N,C) precipitates are initially formed above 1300°C. These particles usually appear associated with inclusions and microssegregation [6,7]. They are called primary precipitates and hardly dissolve under usual slab reheating conditions. After formation of these precipitates, the nucleation and growth of fine particles of (Nb,Ti)(C,N) having different morphologies and Ti/Nb ratios occur. As in the case of primary precipitates, the core of these precipitates is generally richer in Ti and N [6,8-11]. This type of precipitate can be dissolved during the reheating step, resulting in the increase of Nb content in solid solution in austenite before hot rolling process.

There is a large amount of knowledge available in literature [10,12] to estimate the temperature required for the dissolution of Nb-rich precipitates, (Nb,Ti)(C,N), being very common the application of solubility product equations and the use of computational thermodynamics tools, such as Thermo-Calc software. However, these techniques deal only with the thermodynamic aspect, not considering the kinetics, that is, the time required for the dissolution.

Besides that, it is well known that the industrial reheating process is continuous, contrary to the implicit consideration normally assumed in the estimates of isothermal treatment. A further detail is that in most calculations the geometry and size of precipitates formed during the solidification of steel are not considered.

In the present study the effect of reheating temperature on the dissolution of Nb-rich precipitates, under continuous heating conditions close to those practiced in industrial scale, and on the mechanical properties of Ti-Nb microalloyed steel was investigated on laboratory scale. The precipitates dissolution behavior, evaluated by means of transmission electron microscopy, was compared with Thermo-Calc and Dictra simulations.

2 MATERIAL AND METHODS

2.1 Material

The steel used in this investigation was an industrial cast of Ti-Nb microalloyed steel. The C, Nb, Ti and N contents are shown in Table 1.

Table 1. Chemical composition of the microalloyed steel used (wt.%)

C	Nb	Ti	N	Ti/N
0.087	0.019	0.024	0.0035	6.86

2.2 Initial characterization of the precipitates

The characterization of the precipitates formed during the solidification of steel (initial condition) was performed by optical microscopy (OM), scanning electron microscopy (SEM) and transmission electron microscopy (TEM). The analyses

were carried out using samples taken at ½ of the slab thickness in order to obtain the size, morphology and chemical composition of the precipitates. TEM observations were carried out on carbon extraction replicas.

2.3 Characterization of the precipitates after reheating

Samples of 30 mm thickness, taken from slab center, were reheated in an electrical resistance furnace with open atmosphere, according to the curve shown in Figure 1, to varied reheating temperatures. The curve used in the pilot furnace was obtained based on a typical curve [13] employed in the industrial process for the microalloyed steel studied. This industrial curve was reproduced in the pilot furnace in terms of heating rate in the preheating, heating and soaking steps, considering the total residence furnace time applied in the industrial practice. Holding times after the ramps were used to ensure the achievement of the aim temperature values. A thermocouple was inserted in the sample mid-thickness in order to measure the material temperature. After reaching the aim reheating temperature, the samples were quenched in ice water with stirring.
The precipitates characterization was carried out at ½ of the quenched samples thickness by means of TEM and SEM. For precipitate size measurements Aztec software was used.

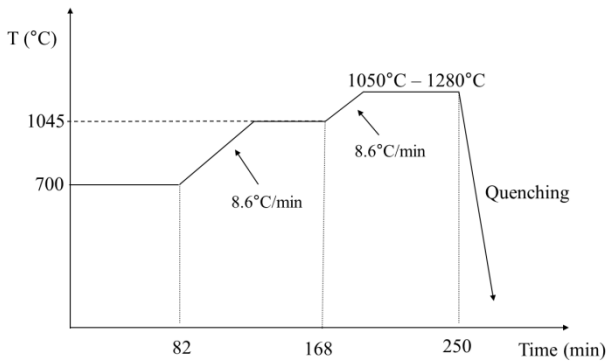

Figure 1. Reheating curve used for ambient temperature in the pilot furnace.

2.4 Kinetics of dissolution during the reheating

The Thermo-Calc software was used for the equilibrium calculations and DICTRA for the diffusion ones, both in the version 2018b. Databases TCFE6 and MOBFE2 were used. The dissolution of carbonitrides was modeled assuming a spherical cell of austenite surrounding a precipitate of carbonitride, also spherical, according to the work by BORBA *et al.* [14].
In the DICTRA simulation, the input parameters were the precipitate and austenitic matrix radii and the chemical composition of the calculated phases in Thermo-Calc, starting from the simplified chemical composition shown in Table 1.
The mean particle radius used was obtained from measurements of the carbonitride diameter distribution using the Aztec software. Three simulations were performed, with different precipitate sizes: 100 nm, which in the as-cast condition represented the highest frequency in the distribution, 280 nm and 500 nm.
The diameter of the austenite cell was calculated so as to match the volume fraction of the two phases, considering the diameter chosen for the precipitate. In the simulation, temperature ranged from 910°C (austenite stability region) to 1280°C, according to the parameters shown in Figure 2. In this case, no holding times after the ramps were used and heating rates were closer to those obtained in the samples heated in the furnace.

2.5 Hot rolling

In order to examine the influence of reheating temperature on the microstructure and mechanical properties of hot rolled plates, pilot hot rolling trials, simulating as close as possible the industrial process, were performed. Samples of 125 mm thickness taken from the center of slab thickness, which is the most critical place in terms of dissolution of precipitates, were heated under the same conditions shown in Figure 1. After discharging, they were hot rolled using

conditions as close as possible to industrial conditions (controlled rolling followed by air cooling). All samples were submitted to the same pass schedule, which resulted in the same final thickness (18 mm).

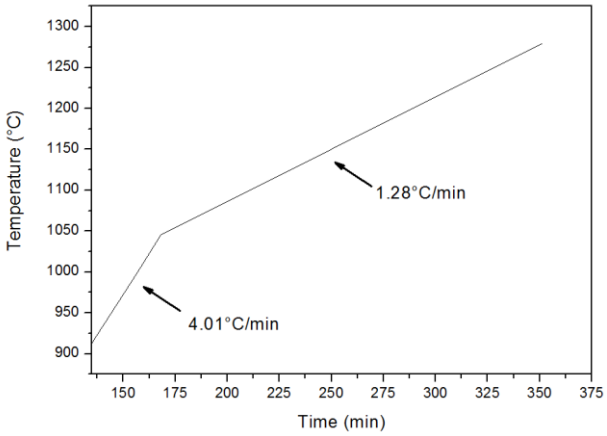

Figure 2. Reheating curve used in the Dictra simulations.

2.6 Microstructural characterization

Longitudinal sections of the rolled plates were prepared following standard metallographic procedures and examined by optical and scanning electron microscopy.

Aiming at quantifying the mean crystallographic unit sizes, electron backscatter diffraction (EBSD) scans were carried out on the hot rolled samples. Apart from mean size, unit size distributions have also been quantified. Different imaging options (inverse pole figure and grain boundary) were analyzed and crystallographic unit sizes were measured considering different misorientation criteria: (i) 4°< ϑ <15° (low angle grain boundaries - D4°): it corresponds to the unit size controlling strength; (ii) ϑ > 15° (high angle grain boundaries - D15°): this unit size is the main feature controlling toughness [15,16]. In addition to quantification of unit size, hardening due to dislocation density has to be considered. In this study, dislocation density has been evaluated from Kernel average misorientation obtained in EBSD. For the quantification of ferrite grain size, the secondary phase (pearlite) has been deleted from the obtained scans.

2.7 Mechanical properties

Tensile specimens with 25 mm gauge length transversal to rolling direction were machined for evaluation of the mechanical properties. The tests were carried out in an electromechanical INSTRON 5882 test machine, at a constant strain rate of 10^{-3}/s.

3 RESULTS AND DISCUSSION

3.1 Programmed and obtained heating curves

A comparison between programmed (furnace temperature) and measured (sample temperature) curves for the samples of 30 mm and 125 mm thickness for a reheating temperature of 1200°C is shown in Figure 3. As can be seen, the measured curves showed three plateaus, corresponding to the preheating, heating and soaking stages. The final temperature reached by the samples in the measured position (center of thickness) was close to target temperature for each stage. As expected, the sample with smaller thickness reached the target temperatures before the larger one. Finally, it is worth noting that the heating rates obtained for each stage are lower than the programmed rates, which justifies the values used for Dictra simulations, Figure 2.

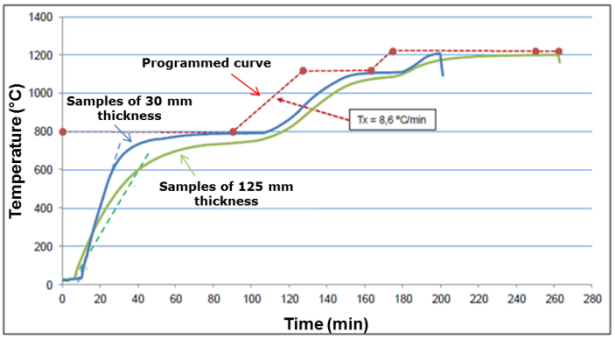

Figure 3. Examples of heating curves obtained with the heating strategy used aiming the discharging temperature of 1200°C.

3.2 Precipitates in slab

Abundant presence of Nb-rich precipitates was verified, often in the form of agglomerates, Figure 4. Cruciform (20-200 nm), rectangular/cubic (20-600 nm), elongated (20-200 nm), needle (more than 500 nm length) and very fine spherical (<10 nm) shaped precipitates were also found. Analyses performed via energy dispersive spectrometer (EDS) showed that the particles were rich in Nb and Ti, with different Nb/Ti ratios, Figures 5 and 6. As mentioned earlier, a higher frequency of Nb-rich precipitate sizes up to 100 nm was observed. Coarse precipitates, larger than 500 nm, were richer in Ti.

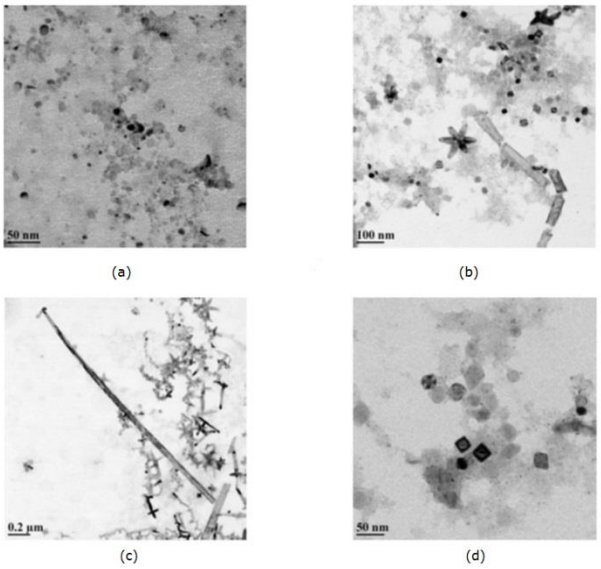

Figure 4. Types of precipitates observed by TEM: (a) agglomerates of fine spherical; (b) Cruciforms, stars and rectangular/cubic shaped; (c) Needle, cruciform and star shaped; (d) Cubic.

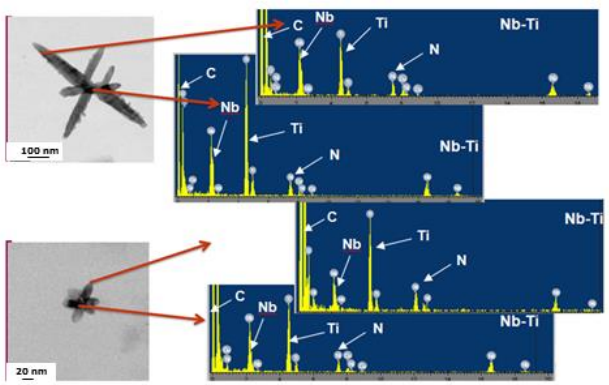

Figura 5. EDS results in cruciform precipitates.

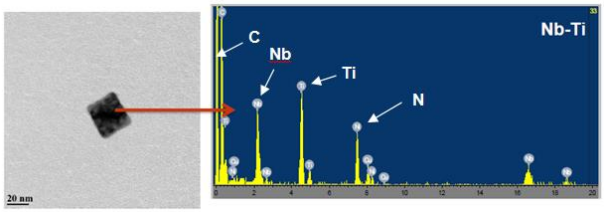

Figure 6. EDS results in a cubic precipitate.

3.3 Precipitates dissolution during the reheating

Images of precipitates observed by TEM are shown in Figures 7 to 10. As can be seen from Figures 7 and 8, a high number of undissolved Nb-Ti rich particles were noticed at the lowest reheating temperatures of 1050°C and 1100°C. Cubic/oval/spherical and cruciform/star/needle shaped precipitates were observed, besides the coarse precipitates richer in Ti and N (primary precipitates). The precipitation state was very similar to the one noticed in the as cast condition. At 1175°C it is possible to note that the cruciform/star/needle shaped precipitates and the very fine spherical precipitates were totally dissolved during the reheating process. Only cubic and rectangular precipitates (>50 nm) were found, besides coarser spherical particles, likely remaining nuclei of cruciform precipitates, Figure 9. Precipitates found at 1200°C were only those cubic shaped with edge size larger than 50 nm (primary precipitates). These particles were observed in an isolated form or in agglomerates. The precipitation behaviors at 1250°C and 1280°C were similar to the one found at 1200°C. Apparently, it seems there was no additional change in form and size of these precipitates. The only change observed was a reduction in the Nb content as the temperature increased, Figure 10.

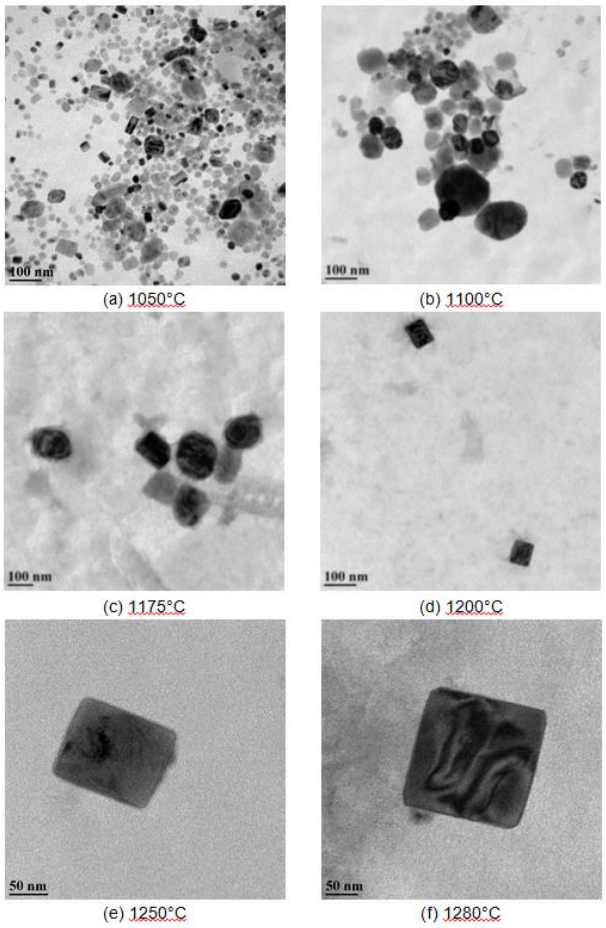

Figure 7. Effect of reheating temperature on Ti-Nb precipitates dissolution.

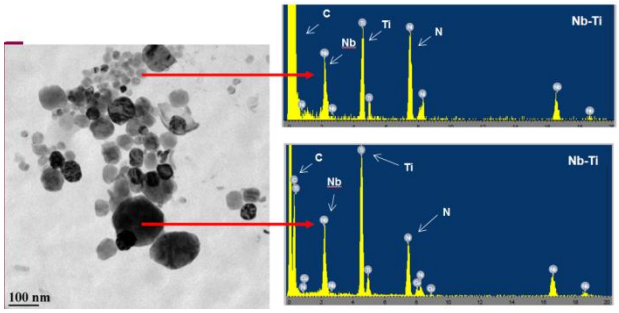

Figure 8. EDS analyses in precipitates found at 1100°C.

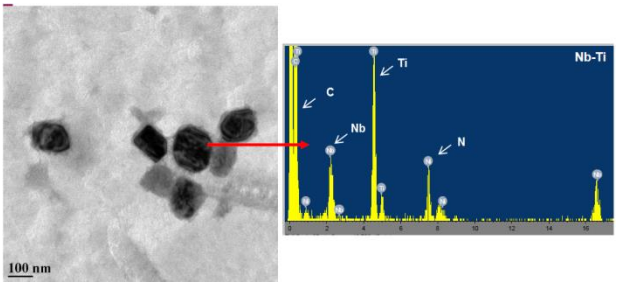

Figure 9. EDS analyses in precipitates found at 1175°C.

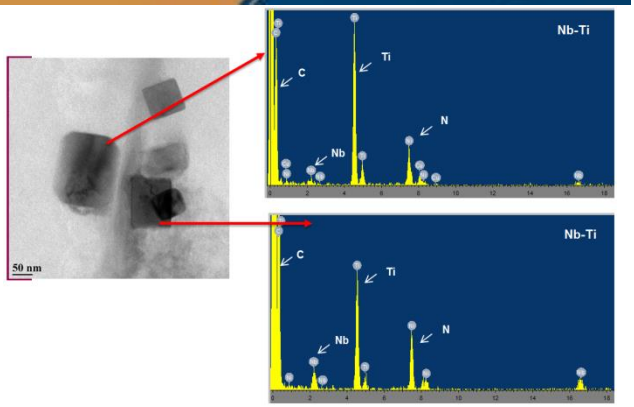

Figure 10. EDS analyses in precipitates found at 1280°C.

3.4 Thermodynamic analysis of precipitation

The temperatures for complete dissolution of Nb and Ti-rich precipitates, (Nb,Ti)(C,N) and (Ti,Nb)(N,C), respectively, are shown in Figure 11. As can be seen, the Nb-rich precipitates dissolve totally, considering equilibrium conditions, at 1108°C. The dissolution occurs almost fully in the austenite stability region. Concerning the (Ti,Nb)(N,C) particles, the dissolution starts around 1140°C and finishes above 1280°C, which was the highest reheating temperature evaluated. According to these results, it can be assumed that the undissolved coarse cubic particles found above 1200°C are primary type precipitates. It can also be concluded, based on the results presented in section 3.3, that during continuous heating the complete dissolution of the Nb-rich precipitates occurs above the equilibrium temperature determined by Thermo-Calc (1108°C).

The distributions of Nb and Ti in the steel studied are shown in Figures 12 and 13, respectively. As can be seen, most of the Nb added to the steel is in the (Nb,Ti)(C,N) form. Thus, when the NbC dissolution is completed almost all the Nb added will be available in solid solution in the austenite (NbAus) for reprecipitation during hot rolling. With regard to Ti, only 17% of the content added to the steel will be available in austenite (TiAus) for reprecipitation.

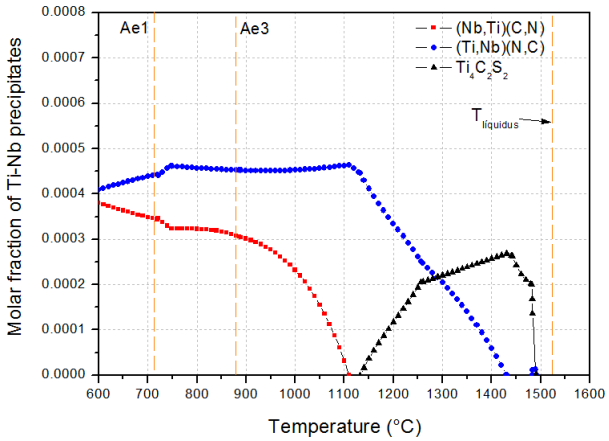

Figure 11. Molar fraction of precipitates with temperature determined by Thermo-Calc software (Thermo-Calc for windows, version 2018b and TCFE6 database).

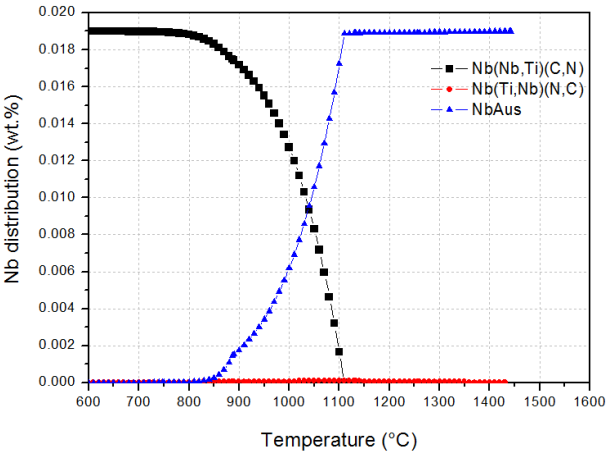

Figure 12. Nb distribution as a function of temperature determined by Thermo-Calc.

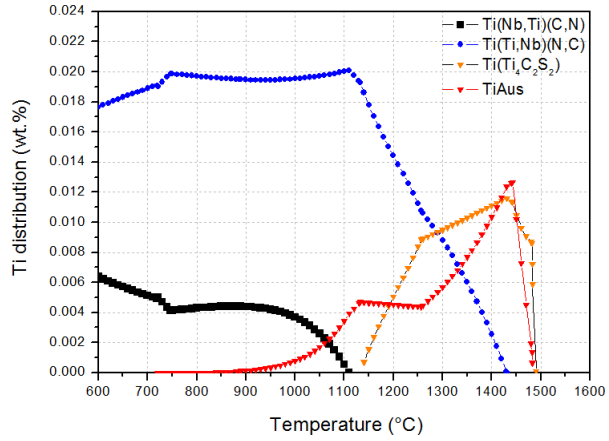

Figure 13. Ti distribution as a function of temperature determined by Thermo-Calc.

3.5 Dissolution kinetics of Nb-rich precipitates

The variations of Nb-rich precipitate diameter and dissolved Nb with time and temperature, calculated with Dictra, are shown in Figures 14 and 15, respectively. As can be seen, for the heating conditions used, the dissolution occurs in the soaking region, above 1000°C, which is in agreement with the Thermo-Calc results. However, the dissolution process does not finish at 1108°C as predicted by Thermo-Calc. For 100 nm diameter precipitates (D_{ppt}), the total dissolution (TD) is reached at 1137°C after 72 min of soaking (t_{soak}), Table 2. Increasing their diameter to 280 nm and 500 nm results in an increase of the TD and t_{soak} required for the complete dissolution. Considering the biggest particle, 500 nm, the complete dissolution is reached at 1228°C after 142 min of soaking, which results in a total furnace residence time (t_{furn}) of 311 min. These results indicate that it is very important to obtain fine Ti-Nb precipitates after steel solidification through adequate alloy design and processing conditions. Thus, the Nb-rich precipitates can be dissolved under usual reheating conditions and the Ti-rich precipitates will, instead, be more effective in restricting the austenitic grain growth.

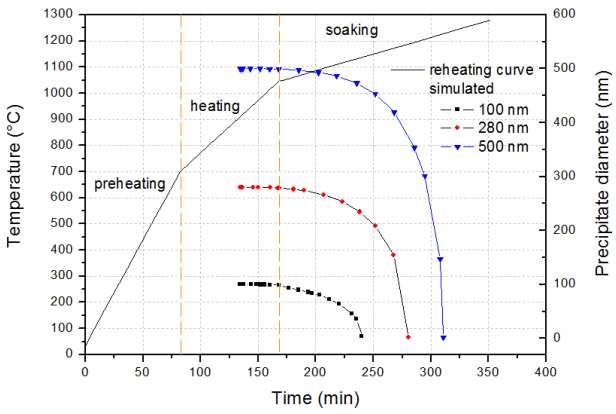

Figure 14. Evolution of Nb-rich precipitate diameter with time and temperature.

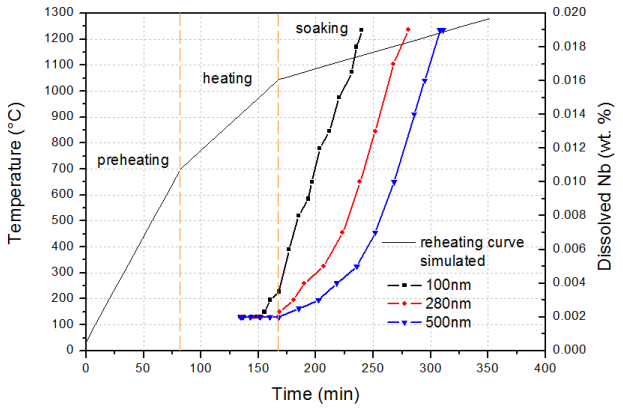

Figure 15. Evolution of dissolved Nb with time and temperature.

Table 2. Reheating conditions for complete dissolution of Nb-rich precipitates.

D_{ppt} (nm)	Complete dissolution		
	TD(°C)	t_{soak} (min)	t_{furn} (min)
100	1137	72 min	240 min
280	1189	112 min	281 min
500	1228	142 min	311 min

3.6 Effect of precipitates dissolution on microstructure

The effect of reheating temperature on microstructure is shown in Figures 16 and 17. Concerning Kernel maps, the color selection done indicates that as the color becomes closer to blue, the dislocation density is lower, while the opposite occurs when more yellow-red color areas appear. Therefore, ferritic recrystallized grains should have quite close to blue-green color. As can be seen in these figures, there is a reduction of D4° with increasing reheating temperature up to 1200°C. After that, an opposite behavior is observed. On the other hand, D15° decreases continuously as the reheating temperature increases.

In the sample reheated to 1200°C, different ferrite populations are observed in the final microstructure. Combinations between non-deformed and deformed ferrite are clearly distinguished both in EBSD scans and optical micrographs. High fraction of deformed ferrite can be observed in the grain boundary map shown in Figure 17, which is characterized by a significant presence of substructure (low angle boundaries represented in red). This suggests that the deformation was applied in the intercritical γ/α region, introducing significant differences in the final microstructure and mechanical behavior.

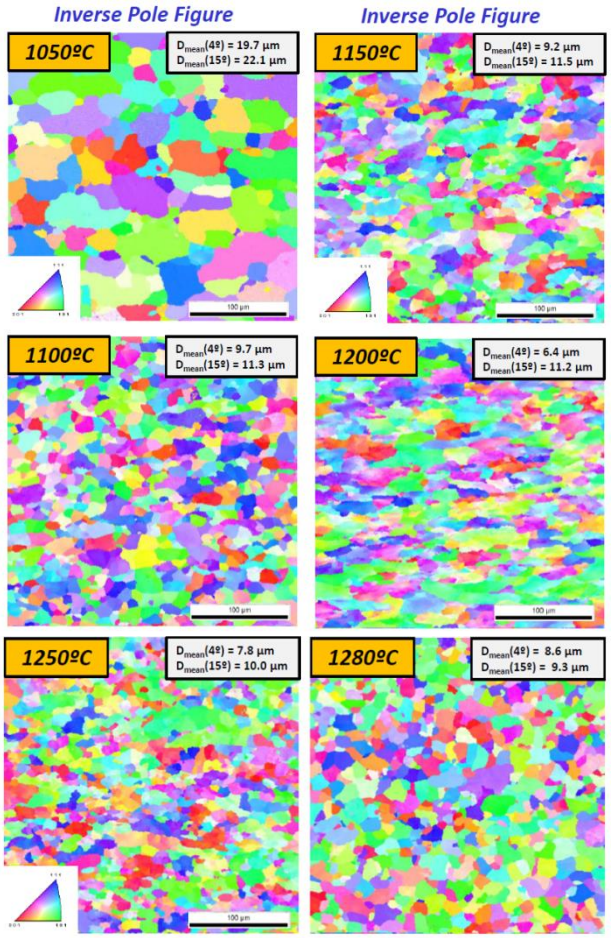

Figure 16. Inverse pole maps of hot rolled samples reheated to different temperatures.

The accumulated area fraction of D4° and D15° is shown in Figure 18. As can be observed, the increase of reheating temperature raised the area fraction of D4°, which can be associated to the Nb precipitates dissolution behavior. Concerning D15°, there is also a trend of raising it as the reheating temperature increases, except at 1200°C due to the presence of non-deformed ferrite in the microstructure. As mentioned before, for toughness the D15° average grain size and volume fraction are the most important factors. So, for a good balance between strength and toughness the intercritical rolling should be avoided.

The variation of mean grain size with reheating temperature is shown in Figure 19. The reduction of the reheating temperature promoted the formation of coarser microstructures. This could be associated with lower contents of Nb in solid solution as the reheating temperature decreased.

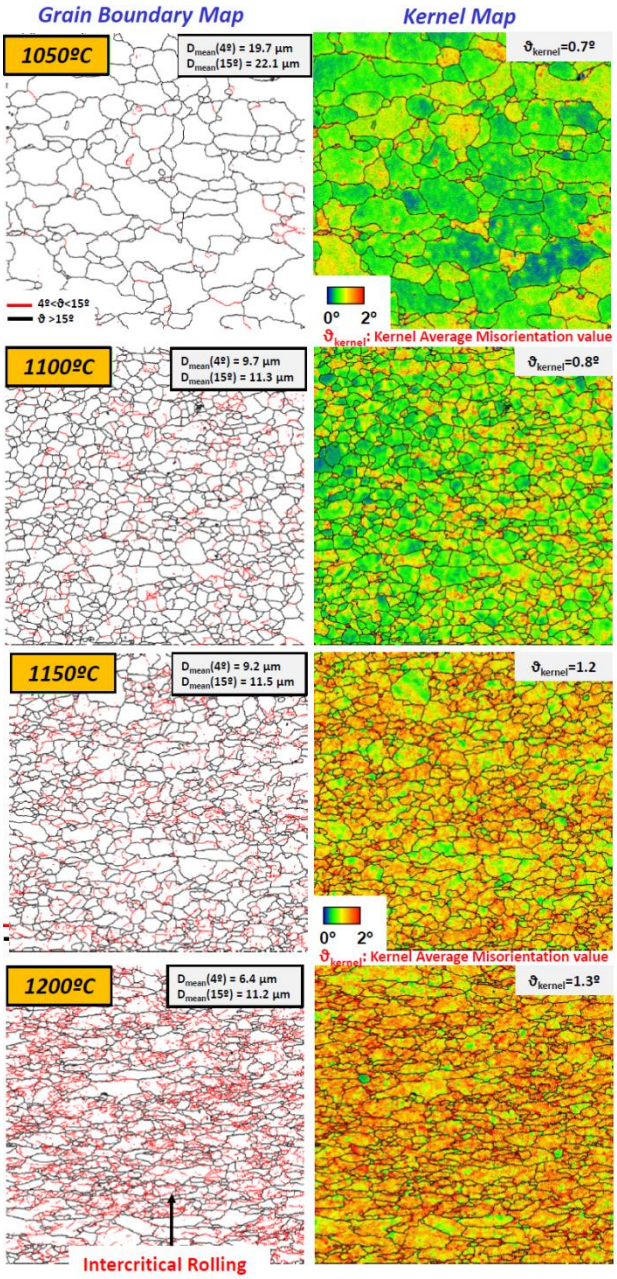

Figure 17. Microstructure of the hot rolled samples reheated to different temperatures.

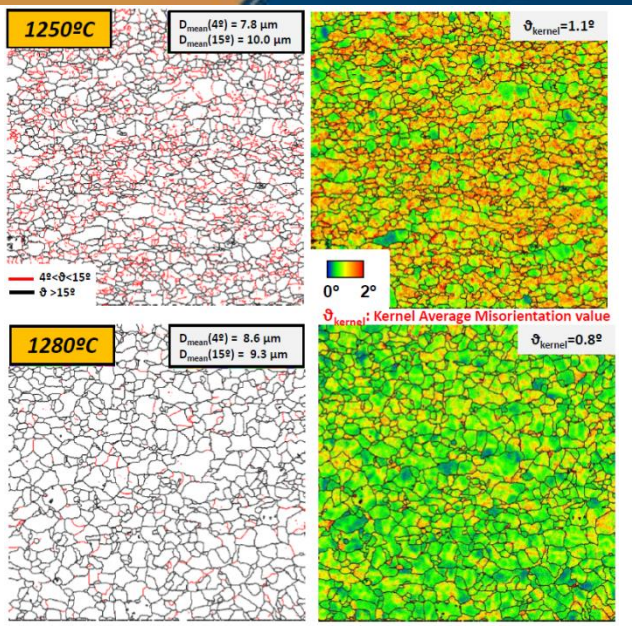

Figure 17. Continued.

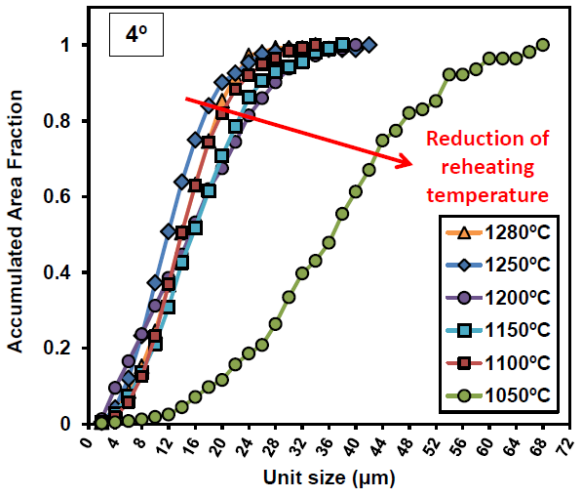

(a)

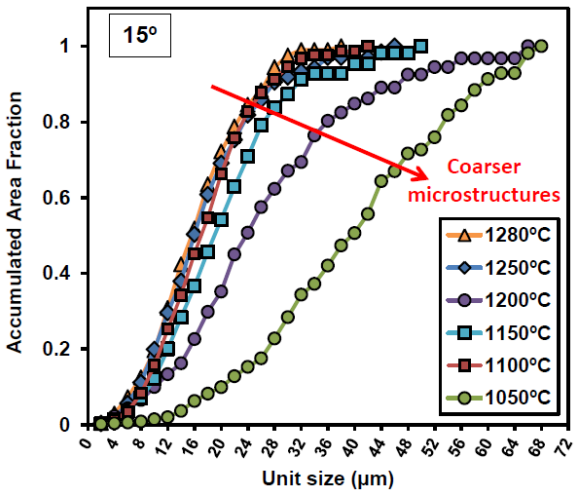

(b)

Figure 18. Effect of reheating temperature on accumulated area fraction of D4°, (a), and D15°, (b).

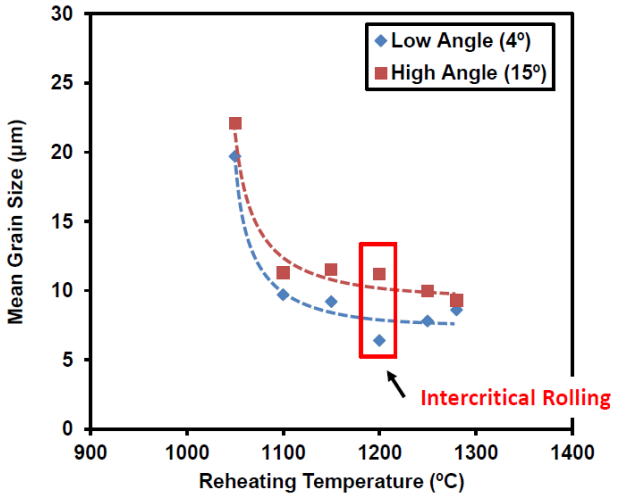

Figure 19. Effect of reheating temperature on mean grain size.

3.7 Effect of the precipitates dissolution on the mechanical properties

The effect of reheating temperature on mechanical properties can be observed in Figure 20. The yield strength and the tensile strength increased with temperature up to 1200°C, due to dissolution of Nb and subsequent fine reprecipitation during hot rolling. At 1200°C the presence of deformed ferrite on the microstructure contributed to the additional increase of strength. It is worth noting an increase greater than 100 MPa in the yield and tensile strength values from 1050°C to 1200°C. Further increase in reheating temperature resulted in strength drop, which may have been caused by the absence of deformed ferrite grains and also by a small increase in D4° average grain size. Concerning the total elongation, the lowest value is observed at 1150°C followed by an increase with temperature up to 1250°C. Beyond this, another drop is observed. This behavior does not fully agrees with the yield and tensile strength results. Reduction in total elongation was expected up to 1200°C followed by a small increase up to 1280°C. The reasons for this discrepancy remain to be investigated.

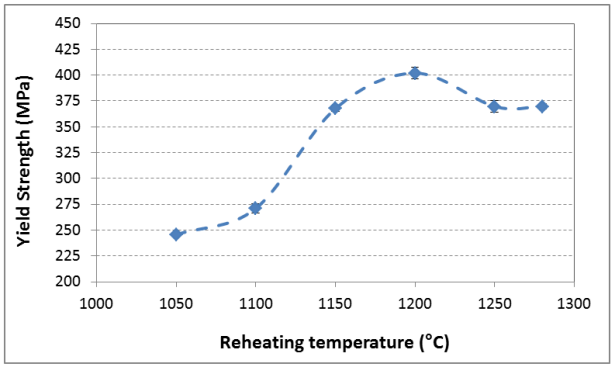

(a)

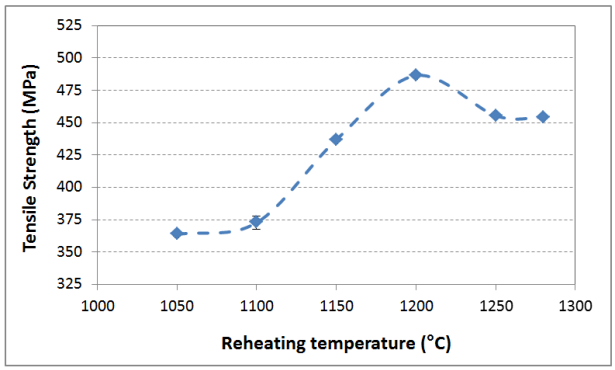

(b)

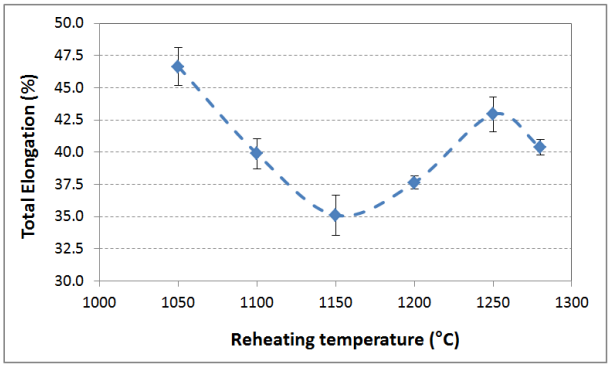

(c)

Figure 20. Variation of yield strength, (a), tensile strength, (b), and total elongation, (c), with reheating temperature.

4 CONCLUSIONS

The dissolution behavior of Nb-rich precipitates in a microalloyed steel was studied in laboratory scale using continuous heating conditions close to those practiced in industrial scale of slab reheating.

It was observed by means of transmission electron microscopy that the dissolution of Nb-rich precipitates occurred almost totally in the soaking region of the reheating

furnace, above 1000°C, and finished in the temperature range 1150°C - 1200°C, which is higher than that predicted by Thermo-Calc software (dissolution temperature equals to 1108°C in equilibrium condition). This is probably due to dissolution kinetic reasons.

In line with these results, the mechanical strength increased with temperature up to 1200°C, due to dissolution of Nb and subsequent fine reprecipitation during hot rolling. The associated refinement of the microstructure also contributed to the increase in strength. Besides that, deformed ferrite in the microstructure of the sample reheated to 1200°C was verified, leading to additional increment in yield and tensile strength. After reheating above 1200°C up to 1280°C, a decrease in strength of the rolled plates was noticed. This effect has been credited to the absence of deformed ferrite grains and to a small increase in the low angle grain boundaries size.

These findings indicate that it is very important to obtain fine Ti-Nb precipitates in the as cast slab condition through an adequate alloy design and processing conditions. This way, the Nb-rich precipitates can be dissolved under usual reheating conditions and the Ti-rich precipitates will be more effective at restricting the austenitic grain growth.

Finally, an attempt to model the kinetics of Nb precipitates dissolution was made using Dictra software, assuming a spherical cell of austenite surrounding a carbonitride precipitate, also spherical. The results obtained were in good agreement with observed precipitates by microscopy and also with mechanical properties obtained of rolled plates. Despite the assumptions, the used methodology allowed to evaluate the effect of steel chemical composition and slab reheating strategy on dissolution kinetics, in order to optimize the use of Nb during hot rolling process.

Acknowledgments

The authors are grateful to the CBMM for support in EBSD and TEM analyses.

REFERENCES

1 Jung HJ, Kang KB, Park CG. Effects of cooling rate and isothermal holding on the precipitation behavior during continuous casting of Nb-Ti bearing HSLA steels. Scripta Materialia, 2003, 49, pp. 1081-1086.

2 Murari FD, Santos AA, Pereda B, Ibabe JMR, Rebellato MA. The effect of soaking time on the dissolution of precipitates and on the mechanical properties of microalloyed steels heavy plates. Rolling and Metal Forming Seminar, ABM, vol. 54, n.54, 2017, São Paulo, pp. 198-209.

3 Murari FD, Santos AA, Gusmão AMR, Pereda B, Lopez B, Rebellato MA. Heating rate effect on the precipitates dissolution and mechanical properties of microalloyed steel plates. Rolling and Metal Forming Seminar, ABM, vol. 55, n. 55, 2018, São Paulo, pp. 525-536.

4 Zheng S, Davis C, Strangwood M. Elemental segregation and subsequent precipitation during solidification of continuous cast Nb-V-Ti high-strength low-alloy steels. Materials Characterization, 95, 2014, pp. 94-104.

5 Nishioka K, Ichikawa K. Progress in thermomechanical control of steel plates and their commercialization. Science and Technology of Advanced Materials. 13, 2012, pp. 1-20.

6 Chen Z, Loretto MH, Cochrane RC. Nature of large precipitates in titanium-containing HSLA steels. Materials Science and Technology, London, v. 3, n. 10, 1987, October, pp. 836-844.

7 Zhou C, Priestner R. The evolution of precipitates in Nb-Ti microalloyed steels during solidification and post-solidification cooling. ISIJ

International, Japan, v. 36, n. 11, 1996, pp. 1397-1405.

8 Carboni MC, Mesquita RA, Cruz EB, Fridman DP, Nogueira MAS. Characterization of precipitates in segregated regions of a Nb bearing API-X70 microalloyed steel. 42nd ABM Steelmaking Seminar, Salvador, 2011, pp. 476-488.

9 Chakrabarti D, Davis C, Strangwood M. Development of Bimodal Grain Structures in Nb-Containing High-Strength Low-Alloy Steels During Slab Reheating, Metallurgical and Materials Transactions A, volume 39A, August, 2008, pp. 1963-1977.

10 Schiavo CP, Gonzalez BM, Santos AA, Marra, KM. Influence of solubilization parameters: soaking temperature and time, on Tnr of microalloyed (Nb, V and Ti) steel. Tecnol. Metal. Mater. Miner., São Paulo, v. 8, 2011, pp. 14-18.

11 Rodriguez-Ibabe JM. The role of microstructure in toughness behavior of microalloyed steels. Mater. Sci. Forum, 284-286, 1998, pp. 51-62.

12 Ding W, Stalheim D, Li S, Bai X, Jiang Z, Li J, Zha C, Li Q, Zhang G. Research and development in the low temperature toughness of large diameter heavy wall X80 pipeline steel at Shougang Steel. Proceedings of IPC 2012. 9th International Pipeline Conference, September 24-28, 2012, Calgary, Alberta, Canada, pp. 249-255.

13 Santos AA, Schiavo CP, Giacomin CN. Computer simulation of slab reheating process in walking beam furnaces. Technology in Metallurgy, Materials and Mining, São Paulo, v. 5, n.1, 2008, pp. 35-39.

14 Borba EC, Castro CSB, Escobar DMP, Murari, FD, Taiss EJM, Silva ALVC, Andrade MS. A study of the dissolution of precipitates during microalloyed steels reheating using computational thermodynamics. ABM Annual Congress, vol. 72, n.1 2017, São Paulo, pp. 2054-2063.

15 Isasti N, Jorge-Badiola D, Taheri ML, Uranga P. Microstructural Features Controlling Mechanical Properties in Nb-Mo Microalloyed Steels. Part I: Yield Strength, Metall. Mater. Trans. A, Vol. 45A, 2014, pp. 4960-4971.

16 Uranga P, Isasti N, Rodriguez-Ibabe JM, Stalheim D, Kendrick V, Frye B, Rebellato M. Optimized Cost-Effective Production of Structural Hot Rolled CSP Coils through Proper Austenite Conditioning, Proceedings of AISTech 2017", Nashville, TN, USA, 2017.